Title: Regulating the femtosecond excited-state lifetime of a single molecule

Authors: K. R. Rusimova[1], R. M. Purkiss[1], R. Howes[1], F. Lee[1], S. Crampin[1,2], P. A. Sloan[1, 2,*].

Affiliations:

[1]Department of Physics, University of Bath, Bath, BA2 7AY, UK.

[2]Centre for Nanoscience and Nanotechnology, University of Bath, Bath, BA2 7AY, UK.

*Correspondence to: p.sloan@bath.ac.uk

Abstract: The key to controlling reactions of molecules induced with the current of a scanning tunneling microscope (STM) tip is the ultrashort intermediate excited ionic state. The energy and position of the injected current sets the initial condition of the excited state, thereafter its dynamics determines the reaction outcome. We show that an STM can directly and controllably influence the excited state dynamics. For the STM-induced desorption of toluene molecules from the Si(111)-7x7 surface, as the tip approaches the molecule, the probability of manipulation drops by two orders of magnitude. A two-channel quenching of the excited state is proposed, an invariant surface channel and a tip-height dependent channel. We conclude that picometer tip-proximity regulates the lifetime of the excited state from 10 to below 0.1 femtoseconds.

One Sentence Summary: Picometer tip proximity of a scanning tunneling microscope quenches single molecule reaction.

Main Text:

Using the tip of a scanning tunneling microscope (STM) to initiate chemical reactions offers a route to controllable single-molecule chemistry (*1*, *2*). Through the mechanical interaction between tip and target molecule, or by the electric field in the gap, the STM can induce molecular change across a ground-state potential energy landscape (*3*). The STM tunneling current, however, can generate excited states of a molecule and hence give enhanced specificity, and more varied outcomes, to the manipulation action, e.g., bond dissociation (*4*, *5*), isomerization (*6*), or tautomerization (*7*). The specificity arises by controlling the energy (*5*) or position (*7*, *8*) of the single electron (or hole) excitation within a single molecule. The ensuing molecular dynamics and hence the final outcome evolve naturally from that point. Having the ability to control and influence the dynamics of the excited-state itself, would open new paths to control matter, and its reactions, at the molecular level.

We find that the lifetime of the positive ion of single toluene molecules on the Si(111)-7×7 surface can be directly controlled by the STM. By bringing the tip close to the molecule (600 to 800 pm), we regulated the excited-state mediated reaction outcome (molecular desorption) by over two orders of magnitude. We correlate this to a reduction of the excited-state lifetime by approximately two orders of magnitude. We propose that a new electronic state is generated by the tip-molecule interaction that provides an additional decay channel for the excited-state, thus quenching the excited-state before its natural surface-limited lifetime elapses. We anticipate this

work to be a starting point for other more complex molecular systems where there are multiple excited-state outcomes where this technique could be used to instigate, probe and control them. The quenching process relies on fundamental quantum processes and should be applicable to a wide class of molecule/surface systems.

Multiple molecular adsorbates have been shown to react to the STM tunneling current (*1*), especially benzene and derivatives (*5*, *9*). Broadly, the probability per electron of inducing a molecular reaction is higher on the Si(111)-7×7 surface than on the Si(100)-2×1 surface, and orders of magnitude higher than on metal surfaces (*7*-*9*). On metals, lifetimes of molecular ion-states are as low as 0.1 fs (*10*), but the reduced density of states in semiconductors lead to longer excited-state lifetimes. The theory of dynamics induced by electronic transition (DIET) links greater lifetimes of excited states to higher probabilities of reaction (such as bond breaking or desorption) (*11*). Benzene, chlorobenzene, and toluene on Si(111)- 7×7 have all been extensively studied (*5*, *9*), and are highly sensitive to tunneling current.

Figure 1 shows a series of STM images charting the positive ion resonance (or negative-bias "hole") induced manipulation of a single chemisorbed toluene molecule on the Si(111)-7×7 surface. At the imaging conditions used (+1 V, 100 pA) chemisorbed toluene molecules were unperturbed by the STM (*12*) and appeared as dark features against the bright spots that were the adatoms of the silicon surface. Chemisorbed toluene molecules formed a 2,5-di-σ bonding configuration with the surface, forming one covalent bond to a silicon adatom (colored red) and one to a neighboring silicon rest atom (second layer atoms with dangling bonds) (Fig. 1A). To manipulate the molecule, during a raster scan from bottom to top, the tip was halted atop the molecule, and current injection was performed (−1.3 V, 900 pA) for 8 s.

Figure 1D shows the tip height variation during this process. In step i, the tip was halted above the molecule. The feedback loop was disabled, and the tip retracted by 1 nm before the voltage was ramped to the desired manipulation value with the set-point current at 20 pA. In step ii, the feedback loop was then re-engaged. In step iii, the set-point current changed to the required injection current, resulting in the tip approaching the surface closer than its initial value by an amount Δz_I. Charge-injection continued, and in this particular case, after 0.35 s of charge injection, the molecule-adatom bond was broken leading to desorption. The underlying (bright) silicon adatom was exposed, causing the tip to withdraw by Δz_M to restore the set-point current (step iv). Resuming the interrupted image scan of Fig. 1B resulted in a "half-moon" feature at the molecular adsorption site typical of a manipulation event occurring mid-scan. Subsequent image scans (Fig. 1C) had the conventional Si(111)-7×7 surface appearance, including the silicon dangling bond at the original location of the toluene molecule.

From the fraction of ~ 120 toluene molecules that were manipulated after an injection time t, we deduced a time-dependent probability of manipulation $P(t)$ for a single-molecule consistent with

the first-order rate equation $dP(t)/dt = k\,[1 - P(t)]$, where k is the rate of manipulation. Figure 2A illustrates this for injection parameters of +1.6 V, 450 pA. Figure 2B illustrates how the manipulation rate k varied with tunneling current for electron injection at +1.6 V. Figure 2C presents data for hole injections at −1.3 V and at −1.0 V. For electron injection, the rate increased linearly with injection current (see fit to Fig. 2B). For hole-injection at low current (2 to 10 pA) we again found a linear dependence, but beyond 10 pA the rate of manipulation was approximately constant; the fitting function of Fig. 2C is discussed below.

The number n of electrons (or holes) that drive a single-molecule manipulation (*4*) leads to a power-law dependence of the rate k with current I, $k \propto I^n$. Hence, for electron injection, the near linear dependence $n = 0.8 \pm 0.1$ indicates a one-electron process (*9*). Similarly, at low-currents a one-hole process is responsible for desorption. However, for hole-injection at currents above 10 pA, the near constant rate implies a largely current-independent process. If the current is not driving the manipulation, what does?

The manipulation rates observed were a factor of 10^4 greater than those occurring in purely thermally-driven desorption of toluene from Si(111)-7×7 (*12*). Hence, the presence of the STM tip is required for this manipulation to take place. Possible tip-molecule interactions that might drive manipulation are mechanical, i.e. a short-range chemical interaction between tip and molecule, or result from the electric field of the tunnel junction. However, we can rule out both. Figure 3A shows the tip-height z during the electron and hole injections performed at different currents. The tip height z is the distance from the center of the bonding Si adatom to the center of the leading atom of the STM tip - see methods. In all cases, z exceeds 600 pm. To identify possible mechanical manipulation, we modified the manipulation experiments by setting the bias during step ii to 0 V, disabling the feedback loop, and setting z to a specific value (schematic, Fig. 3B). For each z value, we then measured the outcome of ~ 90 single-molecule manipulation experiments with an 8-s “exposure” of each target molecule. Little or no desorption was observed for z at or above 600 pm (shaded portion of Fig. 3B). Thus, in the height regime of the current-manipulation experiments, no mechanical manipulation occurred, and the desorption that did occur was consistent with that expected for a thermally-driven process (see Supplementary Materials for $z < 600$ pm discussion).

We eliminated the possibility of an electric-field induced manipulation mechanism by modifying step ii so that, with feedback disabled, the tip retracted an additional distance from the surface. We applied a −10 V bias to generate an electric field $E \approx V/z$ in the junction comparable to that in the current-injection experiments, and whose magnitudes are shown in Fig. 3C. In this case, however, there was no current. As shown by the data presented in Fig. 3D, without the current, there was little or no manipulation.

A similar linear to constant rate crossover appears in two previous works (*13, 14*). There, tip induced band bending (TIBB) was put forward as a possible explanation. Since then detailed theoretical work and scanning tunneling spectroscopy shows that TIBB only occurs if the semiconductor is in depletion (*15, 16*). For our work with n-type Si this would be for electron injection. Therefore TIBB cannot explain our hole injection results nor the results of (*13*). The doping level here and in (*14*) also preclude any significant TIBB even if in the depletion regime (*17*). Instead the model proposed here is consistent with all three reports.

The final outcome of the molecular manipulation can be either that the molecule completely left the surface (desorption), or that it reattached to the surface elsewhere (diffusion). We label an outcome as diffusion if, in an "after" STM image, e.g. Fig. 1C, the manipulated molecule appeared at an adjacent binding site. All other manipulation outcomes are classified as desorption. For all injection currents used, we found a branching ratio B of the probability of desorption to diffusion that was constant throughout the hole-injection experiments, $B_h = 0.037 \pm 0.004$. It was also constant for electron injections with $B_e = 0.24 \pm 0.03$ over the reported range of currents. Furthermore, there is no evidence of other forms of manipulation, e.g., intramolecular bond dissociation (*5*), in either current regime.

Recasting the rate of manipulation in terms of the probability per injected charge of manipulation (electron or hole), $P_e = ke/I$ where e is the magnitude of the electron charge, yields P_e as a function of the tip height z during the current injections. For electron injection, as expected for a one-electron process (Fig. 4A) P_e was fairly constant over the range of z studied. For −1.3 V hole injection, Fig. 4B, P_e dramatically increased with z (i.e., decreasing current), until at ~ 800 pm, we found a near-constant region. Figure 4C shows data for −1.0 V hole injections (10 to 900 pA), where for all injections, we found the same dramatic increase in the manipulation probability as the tip withdrew from the surface.

The desorption of toluene, via a DIET process, follows a three-step process (*18*): (i) Excitation by capture of the injected charge by the toluene molecule; (ii) Dynamics, the evolution of the ionic molecule on its excited state potential; (iii) Detachment, with decay of the state (neutralization) leaving a vibrationally excited neutral molecule and leading to molecule-surface bond breaking and the final outcome of desorption or diffusion. Given that for the same z change, P_e was constant for electron injection, we conclude that step i was also constant for hole injection. That is, the change in the "spot size" of the tunneling current caused by the change in the z must be insignificant and did not change the fraction of the current captured by the molecule. Given the invariance of the branching ratio B_h we further conclude that step iii was the same for all the experiments presented in Fig. 4B. Within a DIET model, what remains to influence the probability of manipulation is step ii, specifically, the lifetime of the excited state (*19*).

For the similar system of benzene on Si(100), Alavi *et al*. (*20*) identified a hole excited-state lifetime of ~ 10 fs and a probability per hole injection similar to our findings. Further, in line with theoretical predictions for long-lived excited states (*19*), Alavi *et al*. reported a monotonic and near linear dependence of the manipulation probability on the hole excited-state lifetime. Therefore, for our hole injections we relate our maximum (i.e. constant region) manipulation probability per hole of $(320 \pm 10) \times 10^{-9}$, with an excited state lifetime of 10 fs, and use the linear dependence, $P_e = \beta\tau$ where $\beta = 32 \times 10^{-9}$ fs^{-1} to map our measured probability of manipulation to an excited state lifetime τ. The result is an excited-state lifetime that changes by two orders of magnitude from 10 fs to below 0.1 fs [see right-hand-side axes of Fig. 4, B and C]. A value of order 0.1 fs is more typical of that of adsorbates on metal surfaces (*10*), indicating that the proximity of the tip transforms the molecule-semiconductor system into a metal-molecule-semiconductor system.

Studies of cyclohexadiene on Si(100) (*21, 22*) have shown the creation of an interface electronic state at the location of the molecule as an STM tip approaches. The new state lies near the Fermi level and in tandem with its creation, the highest occupied molecular orbital (HOMO) at −1.5 V broadened and reduced in intensity as the tip approaches closer. Given our system also contains a π-bonding orbital on a 6-member carbon ring that is di-σ bonded to a Si substrate, we propose that at our higher currents (closest approach) a similar interfacial electronic-state results in the reduced probability per hole of manipulation by providing a new decay channel for the excited molecular which reduces its lifetime and concomitantly the probability of manipulation.

The lifetime of an excited state is the inverse of its relaxation rate $R = 1/\tau$. Here we propose two components for the relaxation of the positive ion state: a fixed rate arising from the presence of the surface $R_S = 1/\tau_S$, with τ_S = 10 fs; and a *z*-dependent rate accounting for the effect of the tip, $R_T(z) = 1/\tau_T(z)$ giving $R = R_S + R_T(z)$. This tip-mediated relaxation channel will be related to the density of states of the interface state, ρ_i , through Fermi's Golden Rule. An analogous scheme is used to describe the STM excitation, direct measurement, and *z*-dependent quenching of the millisecond spin-excitation in single atoms (*23*).

Figure 4D presents schematic energy level diagrams for three regimes of tip-height. (I) large tip-molecule separation with surface dominated excited state relaxation and thus reaction, (II) intermediate-*z* range with onset of an (assumed near the Fermi level) interface state tip-dependent quenching and (III) small-*z* separation with tip-dependent interface state quenching dominating the excited state relaxation. These three regimes are indicated in the rate dependencies of Figs. 4A, B and C.

For a tip-molecule system with localized electronic structure, the force between tip and molecule has been calculated as $F \propto I^m$ with *m* between 1 and 2 (*24*). This calculation invoked a wave function overlap argument and should be broadly similar to the perturbative physics of the initial

generation of an interface state by our STM tip. Thus, we make the connection $R_T(z) \propto \rho_i(z) \propto \exp(-2\kappa z)^m$, leading to a z-dependence of P_e of

$$P_e(z) = \frac{\beta\tau_S}{1+\exp[-2\kappa m(z-z_0)]} \text{ [eq 1]}$$

where $\tau_T(z_0) = \tau_S$ and $\kappa = (1.17 \pm 0.06)$ A^{-1} as found from Fig. 3A. A surface-limited model, $P_e = \beta\tau_s$, has a constant lifetime and so constant manipulation probability. This surface-only model fits the +1.6 V electron injection in Fig. 4A, noting that below ~ 800 pm, there is a possible slight decrease in P_e, suggesting that the negative-ion state is also perturbed by the interface state. For −1.0 V hole injection shown in Fig. 4C, the fit is purely exponential, $P_e(z) \propto \exp(2\kappa z)$, corresponding to a tip-dominated dynamics. For −1.0 V, at all currents, the tip was near the molecule, hence the excited-state dynamics were always tip-limited. At −1.3 V, the tip was slightly further removed from the surface. Thus, Fig. 4B shows a fit to Eq. 1 with $m = 1.1 \pm 0.1$, and demonstrates a cross-over at $z_0 = (830 \pm 20)$ pm from a tip-limited to a surface-limited regime.

Our initial finding of a near invariant rate of manipulation can therefore be reconciled with a 1-hole process. For a 1-hole process the rate is defined as $k = P_eI/e$. Combining this with the tip-dependent manipulation probability P_e of Eq. 1 gives the fit to the rate of manipulation (dashed line) in Fig. 2C. At large tip-molecule separation (low current) the traditional linear $k \propto I$ dependence is evident. For higher currents that led to a closer tip and quenching the molecular excited state, the rate of manipulation became $k = I/I^m = I^{(-0.1 \pm 0.1)}$ giving, as Fig. 2C shows, the largely rate invariant region of manipulation.

Molecules that require more than one electron (or hole) for manipulation, for example C-Cl dissociation of chlorobenzene (*5*) or diffusion of NH_3 (*25*) should naturally be more sensitive to any tip modification of the excited state. We would also expect, alongside other semiconducting molecule/surface systems, any molecule/surface system that displayed long lived excited state, for example molecule/single-atomic-layer-insulator/metal systems (*26*), to be sensitive to tip induced modification of the excited state.

References and Notes:

1. A. J. Mayne, G. Dujardin, G. Comtet, D. Riedel, Electronic control of single-molecule dynamics. *Chemical Reviews* **106**, 4355-4378 (2006).
2. Y. Jiang, Q. Huan, L. Fabris, G. C. Bazan, W. Ho, Submolecular control, spectroscopy and imaging of bond-selective chemistry in single functionalized molecules. *Nature Chemistry* **5**, 36-41 (2013).

3. R. Garcia, A. W. Knoll, E. Riedo, Advanced scanning probe lithography. *Nature Nanotechnology* **9**, 577-587 (2014).
4. B. C. Stipe *et al.*, Single-molecule dissociation by tunneling electrons. *Physical Review Letters* **78**, 4410-4413 (1997).
5. P. A. Sloan, R. E. Palmer, Two-electron dissociation of single molecules by atomic manipulation at room temperature. *Nature* **434**, 367-371 (2005).
6. V. Simic-Milosevic, M. Mehlhorn, K. H. Rieder, J. Meyer, K. Morgenstern, Electron induced ortho-meta isomerization of single molecules. *Physical Review Letters* **98**, 116102 (2007).
7. P. Liljeroth, J. Repp, G. Meyer, Current-induced hydrogen tautomerization and conductance switching of naphthalocyanine molecules. *Science* **317**, 1203-1206 (2007).
8. M. Lastapis *et al.*, Picometer-scale electronic control of molecular dynamics inside a single molecule. *Science* **308**, 1000-1003 (2005).
9. K. R. Rusimova, P. A. Sloan, Molecular and atomic manipulation mediated by electronic excitation of the underlying Si(111)-7x7 surface. *Nanotechnology* **28**, 054002 (2017).
10. L. Bartels *et al.*, Dynamics of electron-induced manipulation of individual CO molecules on Cu(III). *Physical Review Letters* **80**, 2004-2007 (1998).
11. P. Saalfrank, Quantum dynamical approach to ultrafast molecular desorption from surfaces. *Chemical Reviews* **106**, 4116-4159 (2006).
12. D. Lock, S. Sakulsermsuk, R. E. Palmer, P. A. Sloan, Mapping the site-specific potential energy landscape for chemisorbed and physisorbed aromatic molecules on the Si(111)-7x7 surface by time-lapse STM. *Journal of Physics-Condensed Matter* **27**, 054003 (2015).
13. B. C. Stipe, M. A. Rezaei, W. Ho, Site-specific displacement of Si adatoms on Si(111)-(7x7). *Physical Review Letters* **79**, 4397-4400 (1997).
14. X. K. Lu, J. C. Polanyi, J. Yang, A reversible molecular switch based on pattern-change in chlorobenzene and toluene on a Si(111)-(7 x 7) surface. *Nano Letters* **6**, 809-814 (2006).
15. J. Myslivecek *et al.*, Structure of the adatom electron band of the Si(111)-7x7 surface. *Physical Review B* **73**, 161302 (2006).
16. R. M. Feenstra, S. Gaan, G. Meyer, K. H. Rieder, Low-temperature tunneling spectroscopy of Ge(111)c(2x8) surfaces. *Physical Review B* **71**, 125316 (2005).
17. R. M. Feenstra, Tunneling spectroscopy of the (111)-surface of direct-gap III-V semiconductors. *Physical Review B* **50**, 4561-4570 (1994).
18. R. E. Palmer, P. J. Rous, Resonances in electron-scattering by molecules on surfaces. *Reviews of Modern Physics* **64**, 383-440 (1992).
19. P. Saalfrank, G. Boendgen, C. Corriol, T. Nakajima, Direct and indirect DIET and DIMET from semiconductor and metal surfaces: What can we learn from 'toy models'? *Faraday Discussions* **117**, 65-83 (2000).
20. S. Alavi *et al.*, Inducing desorption of organic molecules with a scanning tunneling microscope: Theory and experiments. *Physical Review Letters* **85**, 5372-5375 (2000).
21. B. Naydenov, L. C. Teague, P. Ryan, J. J. Boland, Contact formation dynamics: Mapping chemical bond formation between a molecule and a metallic probe. *Nano Letters* **6**, 1752-1756 (2006).

22. P. M. Ryan, L. C. Teague, B. Naydenov, D. Borland, J. J. Boland, Emergence and visualization of an interface state during contact formation with a single molecule. *Physical Review Letters* **101**, 096801 (2008).
23. W. Paul *et al.*, Control of the millisecond spin lifetime of an electrically probed atom. *Nature Physics* **13**, 403-407 (2017).
24. P. Jelinek, M. Ondracek, F. Flores, Relation between the chemical force and the tunnelling current in atomic point contacts: a simple model. *Journal of Physics-Condensed Matter* **24**, 084001 (2012).
25. J. I. Pascual, N. Lorente, Z. Song, H. Conrad, H. P. Rust, Selectivity in vibrationally mediated single-molecule chemistry. *Nature* **423**, 525-528 (2003).
26. J. Repp, G. Meyer, S. Paavilainen, F. E. Olsson, M. Persson, Imaging bond formation between a gold atom and pentacene on an insulating surface. *Science* **312**, 1196-1199 (2006).
27. S. Sakulsermsuk, P. A. Sloan, W. Theis, R. E. Palmer, Calibrating thermal and scanning tunnelling microscope induced desorption and diffusion for the chemisorbed chlorobenzene/Si(111)7 x 7 system. *Journal of Physics-Condensed Matter* **22**, 084002 (2010).
28. A. S. Lucier, H. Mortensen, Y. Sun, P. Grutter, Determination of the atomic structure of scanning probe microscopy tungsten tips by field ion microscopy. *Physical Review B* **72**, 235420 (2005).
29. D. Lock, K. R. Rusimova, P. A. Sloan, Time lapse recording of automated experiment: https://youtu.be/IuxIyE-nZHc. 2016.
30. Y. Cao, J. F. Deng, G. Q. Xu, Stereo-selective binding of chlorobenzene on Si(111)-7x7. *Journal of Chemical Physics* **112**, 4759-4767 (2000).
31. P. A. Sloan, S. Sakulsermsuk, R. E. Palmer, Nonlocal Desorption of Chlorobenzene Molecules from the Si(111)-(7 x 7) Surface by Charge Injection from the Tip of a Scanning Tunneling Microscope: Remote Control of Atomic Manipulation. *Physical Review Letters* **105**, 048301 (2010).
32. D. Lock, K. R. Rusimova, T. L. Pan, R. E. Palmer, P. A. Sloan, Atomically resolved real-space imaging of hot electron dynamics. *Nature Communications* **6**, 8365 (2015).
33. K. R. Rusimova *et al.*, Initiating and imaging the coherent surface dynamics of charge carriers in real space. *Nature Communications* **7**, 12839 (2016).
34. L. Soukiassian, A. J. Mayne, M. Carbone, G. Dujardin, Atomic-scale desorption of H atoms from the Si(100)-2x1 : H surface: Inelastic electron interactions. *Physical Review B* **68**, 035303 (2003).
35. Z. Majzik *et al.*, Room temperature discrimination of adsorbed molecules and attachment sites on the Si(111)-7 x 7 surface using a qPlus sensor. *ACS Nano* **7**, 2686-2692 (2013).
36. R. Berndt, J. Kroger, N. Neel, G. Schull, Controlled single atom and single molecule contacts. *Physical Chemistry Chemical Physics* **12**, 1022-1032 (2010).
37. M. Utecht, T. Klamroth, Local resonances in STM manipulation of chlorobenzene on Si(111)-7×7: performance of different cluster models and density functionals. *Molecular Physics* **116**, 1687-1696 (2018).

Acknowledgments: We thank Prof Richard Palmer, Prof David Bird and Dr Daniel Wolverson for fruitful discussions. **Funding:** PAS was supported by EPSRC grant EP/K00137X/1. KRR was supported by a University of Bath studentship. RMP was supported by EPSRC CDT CMP grant EP/L015544/1. **Author contributions:** KRR was the primary experimentalist and

performed the analysis. RMP, RH and FL performed sub-sets of the experiments. SC provided theoretic support and data interpretation. PAS led the team, designed the experiment and the analysis. KRR, SC and PAS wrote the manuscript. **Competing interests:** Authors declare no competing interests. **Data and materials availability:** All data supporting this study are openly available from the University of Bath data archive at http://doi.org/xxxxxxxx [To be confirmed].

Supplementary Materials:

Materials and Methods

Supplementary Text

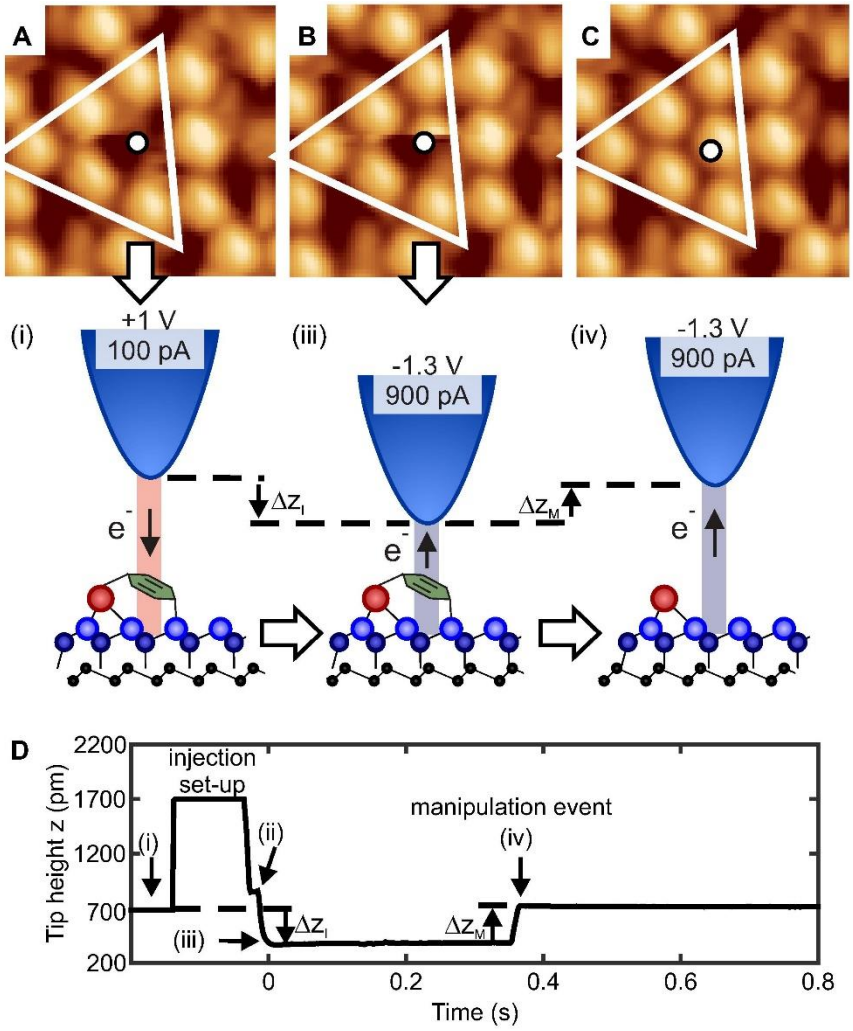

Fig. 1. STM imaging and time-trace of single molecule manipulation. (A to C) High-resolution STM images and (below) corresponding schematic diagrams of the manipulation procedure (imaging parameters +1 V, 100 pA, 3 nm by 3 nm). (A) Before manipulation image: a half unit cell of Si(111)-7×7 is outlined, the white circle atop the missing-adatom like dark spot location indicates the position of a single toluene molecule. (B) During image, (C) after manipulation image. (D) Time-trace of the tip height during manipulation charge injection (see text for details).

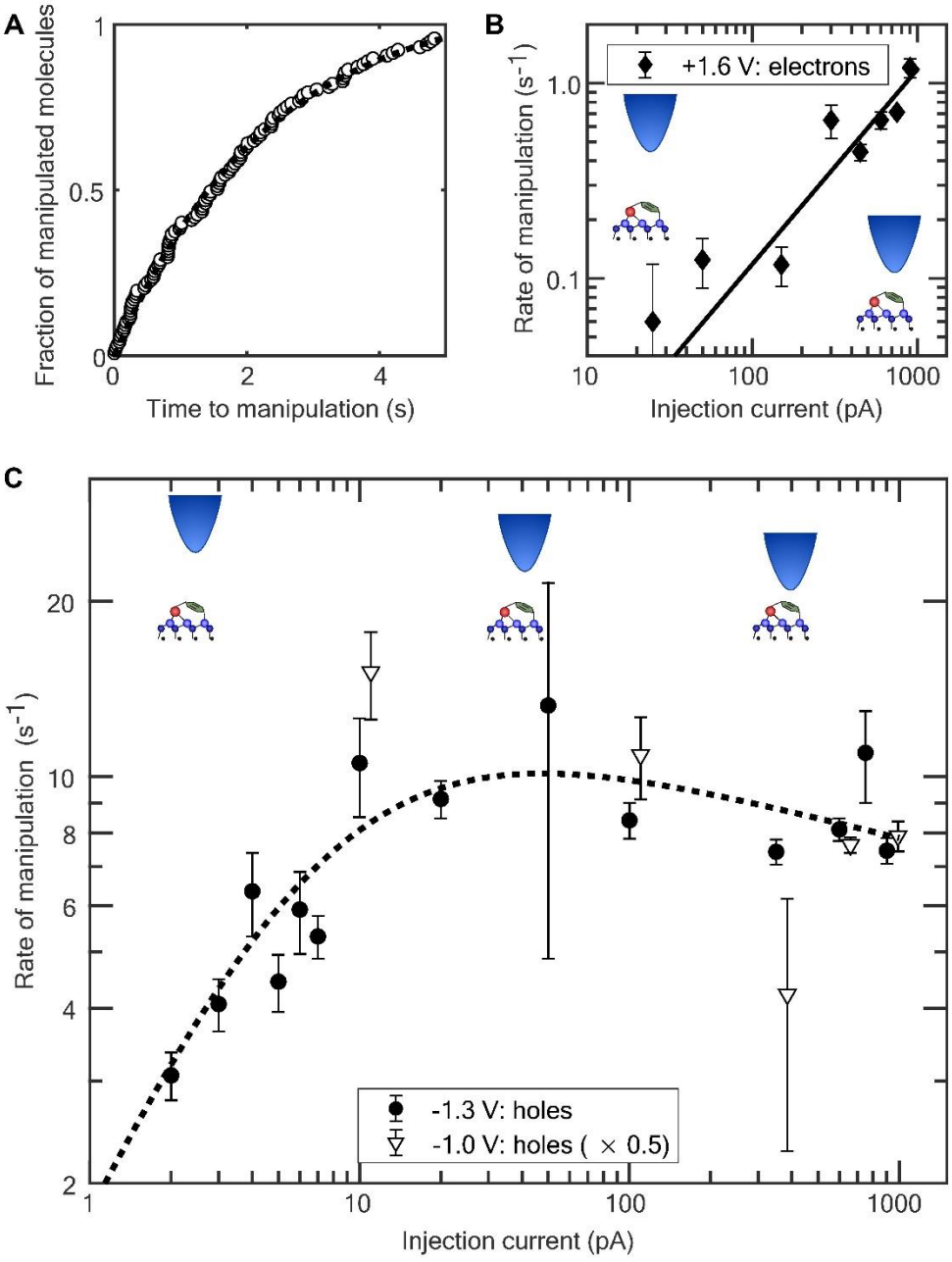

Fig. 2. Rate of manipulation. (a) Time-dependence of the fractional manipulated molecule population (injection parameters +1.6 V and 400 pA; 117 molecules). Also shown is the fit to $P(t) = 1 - e^{-kt}$. (B) Rate of manipulation for electron injection at +1.6 V with a linear fit. (C) Rate of manipulation for hole injection at −1.3 V (filled circles) and at −1.0 V (open triangles). Fit details of tip-dependent model (dashed line) given in main text.

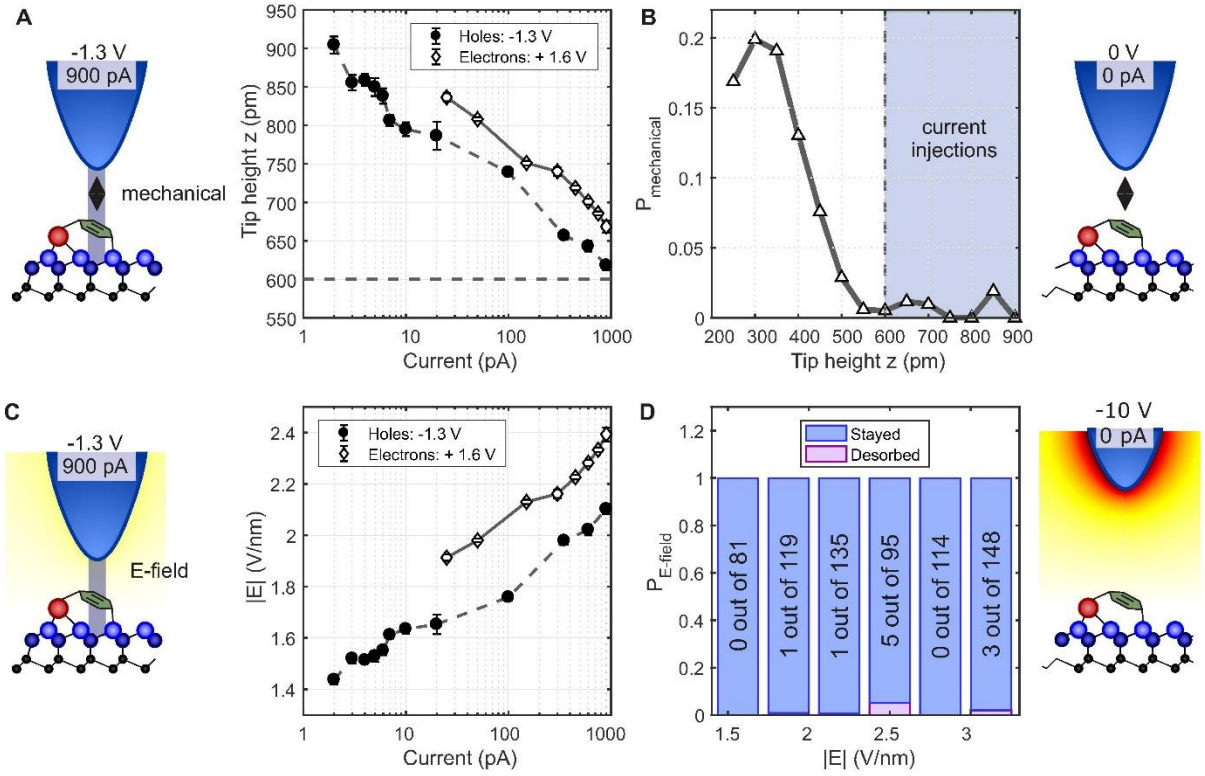

Fig. 3. Mechanical and electric-field tip-induced interactions. (A) Tip-surface separation as a function of tunneling current during charge injection: filled circles, hole injection at −1.3 V; unfilled diamonds, electron injection at +1.6 V. (B) Probability of manipulation after 8 s in the mechanical presence of the tip (0 V, 0 pA). (C) Estimated electric field (magnitude) in the junction between tip and surface as a function of the current *I* during the charge injection manipulation experiments: filled circles, hole injection at −1.3 V; unfilled diamonds, electron injection at +1.6 V. (D) Probability of manipulation after 8 s with only the electric field interaction (−10 V, 0 pA).

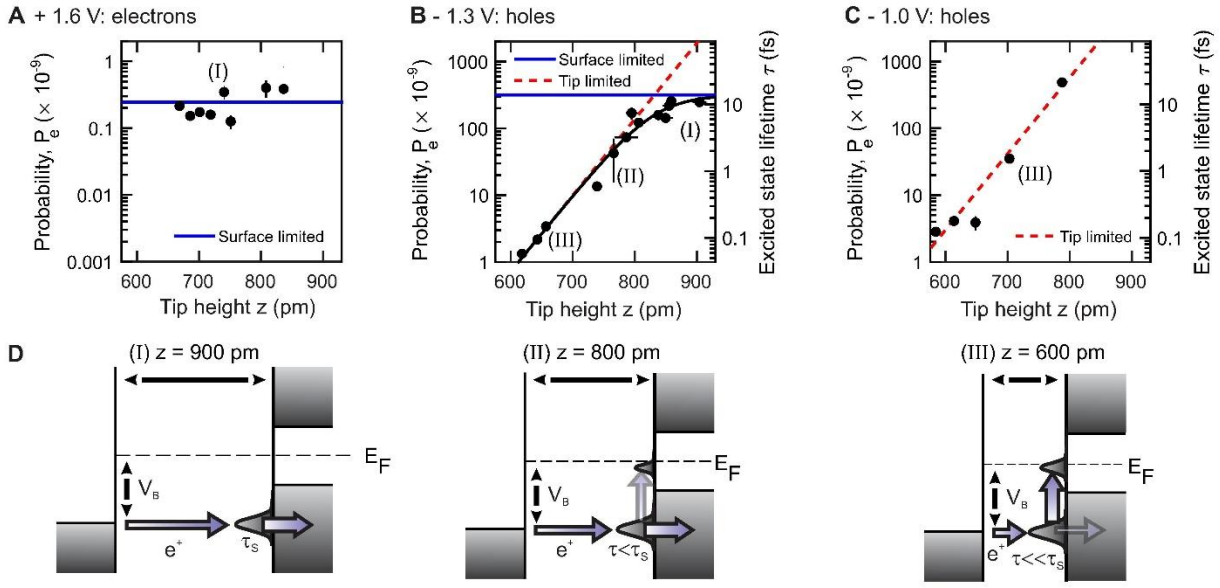

Fig. 4. Manipulation suppression at close tip proximity. (A) +1.6 V electron injection data from Fig. 2B recast as probability per electron as a function of the tip height. Similarly (B) −1.3 V hole injection recast data from Fig. 2C. (C) −1.0 V hole injection. Blue lines show surface limited excited state dynamics, red line models tip-limited dynamics - see text for details. Black curve of (B) is a fit to Eq. 1. Right-hand side axis of (B) and (C) gives the inferred excited-state lifetime τ of the positive-ion with a value of 10 fs for purely surface limited dynamics. (D) schematic energy level diagrams depicting three regimes of tip manipulation suppression – see text for details.

Science
AAAS

Title: Regulating the femtosecond excited-state lifetime of a single molecule

Authors: K. R. Rusimova[1], R. M. Purkiss[1], R. Howes[1], F. Lee[1], S. Crampin[1,2], P. A. Sloan[1, 2,*].

Affiliations:

[1]Department of Physics, University of Bath, Bath, BA2 7AY, UK.

[2]Centre for Nanoscience and Nanotechnology, University of Bath, Bath, BA2 7AY, UK.

*Correspondence to: p.sloan@bath.ac.uk

This PDF file includes:

Materials and Methods

UHV STM

Experiments were performed at room temperature with an Omicron STM1 in an ultrahigh vacuum (UHV) chamber with a base pressure below 1×10^{-10} mbar. Nanonis control electronics was used alongside a suite of LabVIEW programs to automate the experimental procedure, see ref. (*9*). Pre-cut Si(111) samples (n-type, phosphorus doped, 0.001-0.002 Ω cm, 6×10^{19} – 3×10^{19} dopants per cm^3) were reconstructed to form the Si(111)-7×7 surface by repeated high temperature (1250 °C) resistive sample heating (*27*).

Tungsten tips were etched in a 2 M NaOH solution and out-gassed in vacuum to remove any tungsten-oxide (*28*). Toluene was purified by the freeze-pump-thaw technique with liquid nitrogen and checked for purity with a quadrupole mass spectrometer. We chose toluene for this study because of its thermal stability at room temperature, its ease of STM-induced molecular desorption, and its lack of STM current induced intramolecular bond breaking (*9*).

To prepare a partially toluene covered surface (~3 molecules per unit cell) the Si(111)-7×7 surface was dosed through a computer-controlled leak valve. Stability during the injection was ensured by a drift-compensation software (100 fm/s up to 10 pm/s in all 3 directions). All voltages are applied to the sample with the tip grounded through a Femto pre-amplifier.

Automated experiments

To manipulate ~120 individual molecules at each set of injection parameters (tunnel current and bias voltage) we used a home-made LabVIEW control program running in combination with a bespoke MATLAB analysis suite (*27*). Each automated experimental sequence involves the following steps: (1) LabVIEW takes a 25 nm × 25 nm overview image of the silicon surface; (2) MATLAB analyses the image to identify all atomic and molecular locations and randomly picks a user-specified number *n* of injection sites. All selected molecules are located on top of faulted middle silicon adatoms, belonging to different unit cells; (3) LabVIEW moves the STM tip to the first set of x-y coordinates specified by MATLAB. The STM takes a 3 nm × 3 nm image of the surface and performs a cross-correlation with the same region cropped out from the "big" overview image in order to correct for any drift that has occurred in the interim. (4) Once the correct injection location has been established, the STM takes a series of three 3 nm × 3 nm consecutive images, as described in Fig. 1 and the main text; (5) Steps (3) and (4) are repeated *n* times for each set of injection co-ordinates; (6) Finally, the STM takes a 25 nm × 25 nm overview image of the silicon surface after all *n* injection experiments have been performed. Each experimental sequence like this takes about 15-20 min and involves up to 20 individual current injections into single molecules. See ref. (*29*) for a time-lapse video of the automation procedure.

Details of manipulation measurement

Toluene is di-σ bonded to the Si(111)-7×7 surface, forming a covalent bond to a silicon adatom and another to a neighboring silicon restatom (*30*). In line with our previous work (*9*) we only inject into molecules bonded to faulted middle adatoms. Previously we reported on the local

manipulation of the toluene/Si(111)-7×7 system. For electron injection we found two populations depending on their precise chemisorption geometry (choice of two crystollographically equivalent rest-atoms). This resulted in two rates of desorption, dependent upon whether the tip was atop the center of the molecule, or more atop the position of the bonding adatom. The former gave a higher rate of manipulation than the latter. For the experiments reported here, we only report on the faster process for those molecules where the adsorption configuration placed the molecule directly under the tip.

The Si(111)-7×7 exhibits nonlocal manipulation whereby the injected charge flows across the surface and induces molecular desorption some 10 nm distant from the injections site (*31*-*33*). Here, for electrons, our injection voltage of +1.6 V is well below the thresholds for nonlocal manipulation with electrons of +2.0 V (*32*). For the hole injections of -1.3 V, we are just at the onset of hole induced nonlocal manipulation for faulted-middle molecules. At this threshold the nonlocal probability is lower than that reported here for the local manipulations (*33*). The probability of nonlocal manipulation of a FM molecule with -1.3 V injection is given in ref (*33*) as $(4.3 \pm 0.5) \times 10^{-15}$. Nonlocal processes will therefore not influence our single-molecule experiments. The rate of manipulation was determined from the time dependent manipulation probabilities using the methods presented in ref (*32*).

The spread of rate data points in Fig. 2B was consistent with similar STM experiments (*34*), given the inherent uncertainties of the STM tip's chemical composition. To minimize this influence, we monitor the STM images of the Si(111)7x7 surface so they appear as shown in Fig. 1. We also gathered a statistically significant number of manipulation events for each set of injection parameters.

Absolute tip-height

To present absolute tip-heights we correlate the onset of the mechanically induced manipulation shown in Fig. 3B, with the onset of the repulsive force as measured by AFM (*35*) found at 600 pm relative to the center of the bonding silicon adatom.

Supplementary Text

Mechanical Manipulation

Only for $z < 500$ pm did we begin to see evidence for mechanical manipulation, which we attributed to the close approach of the STM tip modifying the neutral potential energy surface of the molecule-surface system by lowering the barrier to desorption or diffusion by ~ 100 meV, which enhanced thermally activated molecular desorption and diffusion . This < 500 pm region mostly likely reflected direct contact between tip and molecule (*36*). Quantitatively, even at the shortest separations, the effective rate of mechanical manipulation is a small fraction ($k_{mech} < 0.03\ s^{-1}$) of that caused by hole-injection, as seen in Fig. 2C.

Possible experimental limitation

For hole injections at the lower voltage of −1.0 V, Fig. 2C, the rate of manipulation was also largely constant over all the currents probed. Because this invariant region had a different rate from the invariant region for −1.3 V, by a factor 2, we discounted the possibility that the plateau is caused by experimental measurement limitation. Moreover, the similar findings of refs (*13, 14*) point to the rate-invariant region being a true measurement and not simply an experimental artefact.

Negative-ion probability invariance.

An interface state situated on the molecule would explain the lack of obvious *z* dependence (Fig. 4A) for electron injections. The negative-ion state is located within the silicon back-bonding orbitals that underlie the bonding molecule-adatom site, whereas the positive-ion state is located on the molecule itself (*9, 37*). Thus, an interface state located on the molecule would have larger Franck-Condon overlap with the positive-ion state then the positive-ion state. This is consistent with the findings here that hole injections are much more sensitive to the tip proximity than electron injections.

Junction electric field

At room temperature the Si(111)-7×7 surface does not exhibit tip-induced band-bending (*15*). The surface acts as a metal. We therefore model the STM *E*-field as that between two spheres with opposite charge q of radius R a distance $2\times z_0$ apart, the surface plane lying at the midpoint defined as $z = 0$. This gives the z dependence of the field as

$$E(z) = \frac{q}{4\pi\epsilon_0}\left[\frac{1}{(R + z_0 - z)^2} + \frac{1}{(R + z_0 + z)^2}\right].$$

To justify the use of the standard parallel plate capacitor form $E=V/z$ we ensure that the E-field in the gap only changes by 10 % across the gap. Solving $E(z_0)/E(0) = 1.1$ for a gap of 0.7 nm gives a minimum radius of the tip as 4.6 nm. Scanning electron microscopy of our STM tips shows that typically they have a radius of curvature of a few tens of nanometers. Therefore the parallel plate capacitor relation $E=V/z$ is well justified.

Furthermore, the work of ref (*21*) shows a constant signal in their STS measurements of the interface state across a range of tip heights. Thus the interface state is unperturbed, or at least has no measureable change induced by the variations of the junction *E*-field.